Journal of Fluids and Structures (1997) **11,** 767–792

APPRAISAL OF A SEMI-EMPIRICAL MODEL FOR THE PRESSURE FIELD BENEATH ROOF CORNER VORTICES

C. W. Williams and C. J. Baker

Department of Civil Engineering, University Park, Nottingham NG7 2RD, UK.

(Received 14 December 1996 and in revised form 17 April 1997)

In 1990 Cook described a semi-empirical model for predicting the pressure field beneath roof corner vortices. He proposed that the flow can be considered as a conical vortex "growth region" near the roof corner, and as a cylindrical vortex "mature region" further away from the corner, and derived an equation for surface pressure based on the supposed mechanics of a Rankine vortex with a number of variable parameters. The work described in this paper sets out to investigate the adequacy of this model. Firstly, three extensive data sets are used to determine the ranges of building geometry and wind direction for which the model is valid, and to determine the model parameters. It is found that the growth region model is a good descriptor of the pressure field for corners of included angle 60° or more, with wind directions between $\pm 15°$, approximately, to the corner bisector. No mature region in the form suggested by Cook was found, although for low height/length ratio buildings a change in flow pattern near the rear of the building was apparent, but not in the form suggested by Cook. The model parameters derived for the growth region were on the whole consistent, and provided useful insights into the mechanics of the vortex system. These parameters were used to predict the measured pressure distributions of a further independent data set and reasonable agreement was found. Future developments and applications of the model are discussed.

1. INTRODUCTION

For low rise buildings with winds at oblique angles to the edges, the existence of "delta wing vortices" in the region of the windward facing corner is well established at both model scale and full scale. These vortices produce potentially damaging high suctions on the roof surface in their vicinity. The precise nature of these vortices is at the moment the subject of considerable investigation, both through measurements made on wind tunnel models [for example, Kawai (1996), Marwood & Wood (1996)] and through the use of various computational fluid dynamics (CFD) techniques [see, for example, the LES calculations of Thomas & Williams (1996)].

It is apparent from the CFD investigations that current CFD codes are not able to adequately model these vortex flows, although work on large eddy simulations is showing some promise. In addition, the wind tunnel work, whilst producing a great deal of high quality experimental data, nonetheless lacks a suitable framework for analysis and comparison between the different data sets. Cook (1990) proposed a semi-empirical model of the pressure field beneath such vortices, based approximately on what would be expected beneath a Rankine vortex. This model contains a number or parameters that need to be determined experimentally. Cook suggests that this model has the potential to be useful in design, if the parameters can be adequately specified, and could also be a useful research

0889-9746/97/070767 + 26 $25.00/fl970102

tool as it provides a framework for the systematic consideration of the effect of changes in, say, building height, turbulence intensity, etc. Cook himself only carried out a superficial calibration of the model, determining the various parameters by a best fit analysis to measured pressure fields.

The present paper considers this model further in a reasonably systematic manner. In Section 2 the model formulation is set out and a physical interpretation given to the various model parameters. Section 3 sets out the data sets used in the analysis–three fairly extensive sets of data that were used to investigate the variation of the various model parameters, and one further independent data set that was used for verification purposes. Section 4 then considers the "mature region" of the model, the region of the vortex well away from the leading corner in which Cook considers the overlying vortex pattern to be a cylindrical vortex parallel to the roof edge. Section 5 then considers the "growth region", near to the vortex corner, where Cook assumes a conical vortex region to exist. The extent of the validity of this model is determined, and the model parameters obtained from the three extensive datasets. Section 6 then attempts to verify these parameters by comparing the predicted results with the results of a further independent dataset. Finally, in Section 7 the adequacy of the model is discussed and some concluding remarks are made.

2. THE SEMI-EMPIRICAL MODEL

2.1. Model Formulation

Figure 1 is a definition sketch of the coordinate system that will be used. It shows the flat roof of a wedge-shaped building with included angle θ (shown here for $\theta = 90°$). The x and y axes are aligned with the cube edges, which have lengths W and L, respectively. The building has a height H; r is the radical distance along a line from the cube windward corner at an angle α to the corner bisector. The wind direction is given by the angle β to the corner bisector. In what follows, the vortex on the side of the cube for which β is positive will be referred to as the windward vortex, and the vortex on the negative β side as the leeward vortex.

In his model Cook essentially assumes two regions of vortex flow. For the first, the growth region, he assumes that a vortex develops along a radial line from the apex, whilst for the second, the mature region, he assumes that after some distance from the apex the vortex ceases to develop and follows a track parallel to the edge of the roof. In the growth region the surface pressure distribution is taken to have the form.

$$C_p = C_{p0} + (C_{p1} - C_{p0})\,[1 - S\log(r/b)]/\{1 + [(\alpha - \alpha_0)/\alpha_c)]^2\} \tag{1}$$

Here C_p is the pressure coefficient at (r, α), and C_{p0}, C_{p1}, S, b, α_0 and α_c are parameters to be determined, whose meaning will be considered in Section 2.2.

In the mature region, the pressure distribution is taken to be given by a similar equation

$$C_p = C_{p0} + (C_{p1} - C_{p0})\,[1 - S\log(r_m/b)]/\{1 + [(y - y_0)/y_c)]^2\} \tag{2}$$

where C_p is the pressure coefficient at a distance y from the edge of the block; r_m, y_0 and y_c are again parameters to be determined.

2.2. Physical Interpretation of Cook's Model

First consider the growth region as defined by Cook. Essentially it is assumed that the pressure coefficient can be taken to vary with distance from the upstream corner, and with

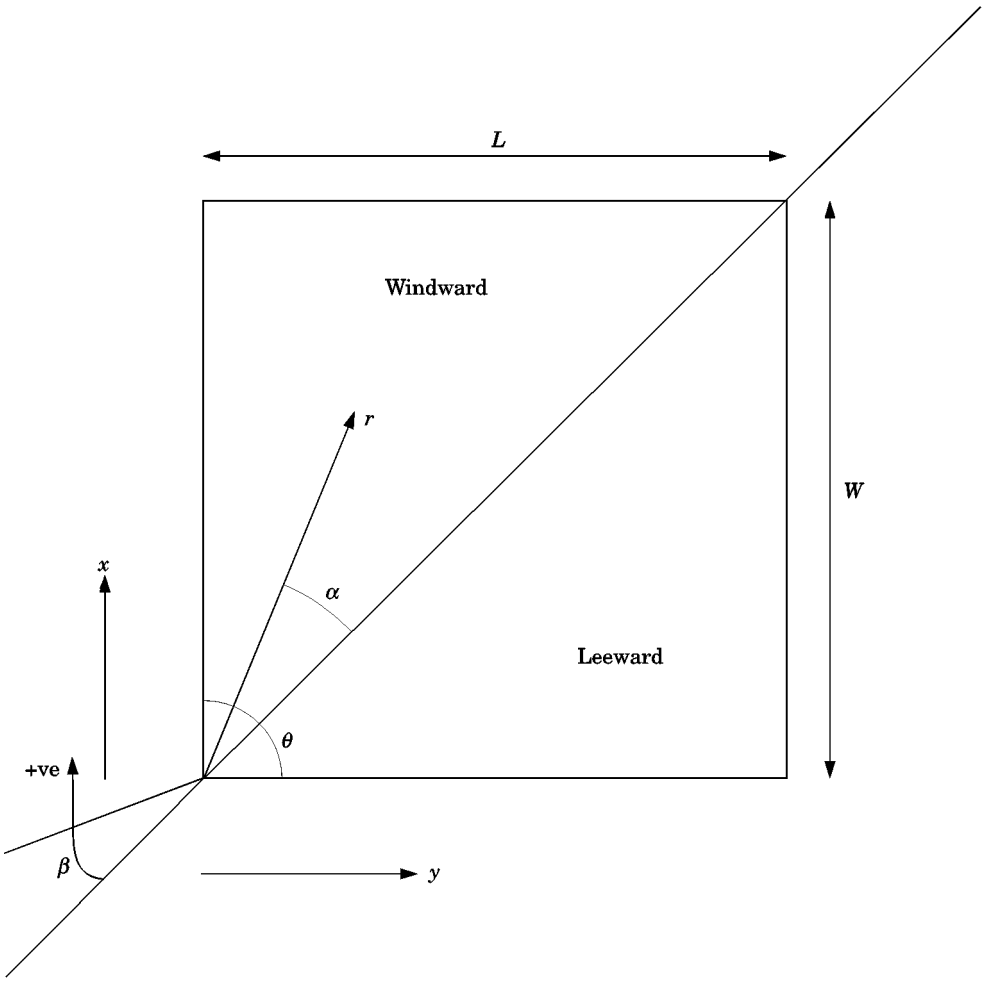

Figure 1. Definition sketch of coordinate system.

angular displacement from some reference angle. The two variations are taken to be independent of each other. The variation with distance from the corner is taken to be logarithmic (based on experimental observations), whilst the angular variation is taken to be given by the term in α in equation (1). Cook argues that the form of this variation is consistent with what would be expected beneath the core of a Rankine vortex (see below). On the line from the corner where $\alpha = \alpha_0$ the pressure is a minimum, and α_0 is to be interpreted as the angular position of the vortex core. α_c is some measure of the radius of the core. b is some arbitrary reference length: in what follows it will be taken as the height of the block or building under consideration. C_{p0} and C_{p1} are reference pressure coefficients with no particular physical meaning. Mathematically, for $\alpha = \alpha_0$ and $r = b$, $C_p = C_{p1}$, and, when α is very large $C_p = C_{p0}$.

In the mature region the vortex track is taken to be parallel to the edge of the building. The pressure is still assumed to vary in the perpendicular direction in the same way, with

y_0 replacing α_0 and y_c replacing α_c, but no variation is assumed along the vortex core. The parameter r_m is the value of r at the end of the growth region.

Before proceeding further it is necessary to consider whether or not the model of Cook is actually representative of the flow beneath a Rankine vortex. The Appendix shows that the "angular" function of equation (1) is not truly representative of the pressure field on a surface beneath a Rankine vortex, but nonetheless it has the correct general behaviour—a maximum at $\alpha = \alpha_0$ and tending towards a constant value for large values of α, and the parameters in that equation are surrogates for perhaps more physically meaningful parameters (such as vortex height above the surface, core diameter and velocity, etc.). It is thus best to think of Cook's model as an empirical representation of the pressure field below a vortex system that would seem to adequately represent reality, rather than a precise description of the flow beneath a Rankine vortex.

Finally it should be noted that, in what follows, Cook's expressions will be written in a slightly different format. For the growth region (which as will be seen is the major region of interest), equation (1) will be rewritten as

$$C_p = C_{p0} + (\Delta C_p - G \log(r/b)]/\{1 + [(\alpha - \alpha_0)/\alpha_c)]^2\} \tag{3}$$

where $\Delta C_p = C_{p1} - C_{p0}$ and $G = S\Delta C_p$.

3. DATA SETS USED IN ANALYSIS AND VERIFICATION

3.1. Analysis

Three extensive data sets were used to find the parameters in Cook's model for a variety of conditions. The experimental conditions under which they were obtained are described in what follows.

3.1.1. Results of Maruta (1985)

Maruta (1985) carried out experiments in the BRE No 2 wind tunnel on a series of wedge-shaped blocks of included angle θ of 30, 60, 90 and 120°. The blocks were of length $L\,(= W)$ equal to 0·1 m and were tested at heights (H) of between 0·05 m and 0·2 m, giving values of L/H between 0·5 and 2·0. However, all the results presented here are for $L/H = 1{\cdot}0$. For each wedge, the wind angle β was varied between 0° and normal to one face of the block. The atmospheric boundary layer simulation has a roughness length of around 0·001 m, and the wind tunnel mean velocity at the height of the top of the block was 10 m/s. Values of turbulence intensity and length scale are not given. The data was analysed in the standard BRE manner to produce mean and extreme pressure coefficients at each tap. The mean pressure coefficients were normalized with the mean velocity, and the extreme pressure coefficients obtained from a conventional Gumbel extreme value analysis for sampling periods of 0·01, 0·04 and 0·16 s were normalized with the extreme value of velocity for a corresponding time period [the pseudo steady form defined by Cook (1985)]. Assuming a geometric scale of 1/100th and a velocity scale of unity, these correspond to 1, 4 and 16 s extreme values, which are classified in BRE terms as class A, B and C values. Only mean values and class A values will be discussed in this paper.

3.1.2. Results of Williams (1995)

Williams (1995) describes tests carried out in the BRE No 3 wind tunnel on a cuboid ($\theta = 90°$) with $L = W = 0{\cdot}6$ m and values of H of 0·075, 0·15, 0·2, 0·3 and 0·6 m, giving

values of L/H of 1, 2, 3, 4 and 8. However results for $L/H = 8$ will not be discussed here to any extent, since for this situation the height of the top of the block was similar to the height of the upstream surface roughness elements, and it was felt that the measured pressures could have been affected by the wakes of individual roughness elements (particularly near the leading edge). The block was extensively pressure tapped with a large number of taps in the windward corner (Figure 2). Wind angles β of 0 and 15° were used. The atmospheric boundary layer simulation had a surface roughness length of 0·007 m and a displacement height of 0·025 m, with values of the longitudinal turbulence length scale of between 0·3 m and 0·5 m. The turbulence intensities at heights of 0·15, 0·20, 0·30 and 0·6 m (i.e. the various block roof heights) were 0·26, 0·22, 0·18 and 0·10, respectively. Thus, note that in these experiments the block height/length ratio and the rooftop turbulence intensity vary together. The wind tunnel velocity at a height of 0·3 m was 14·5 m/s. Mean pressure coefficients and class A, B and C pressure coefficients were measured as in the tests of Maruta. Again, only mean and class A coefficients are considered here.

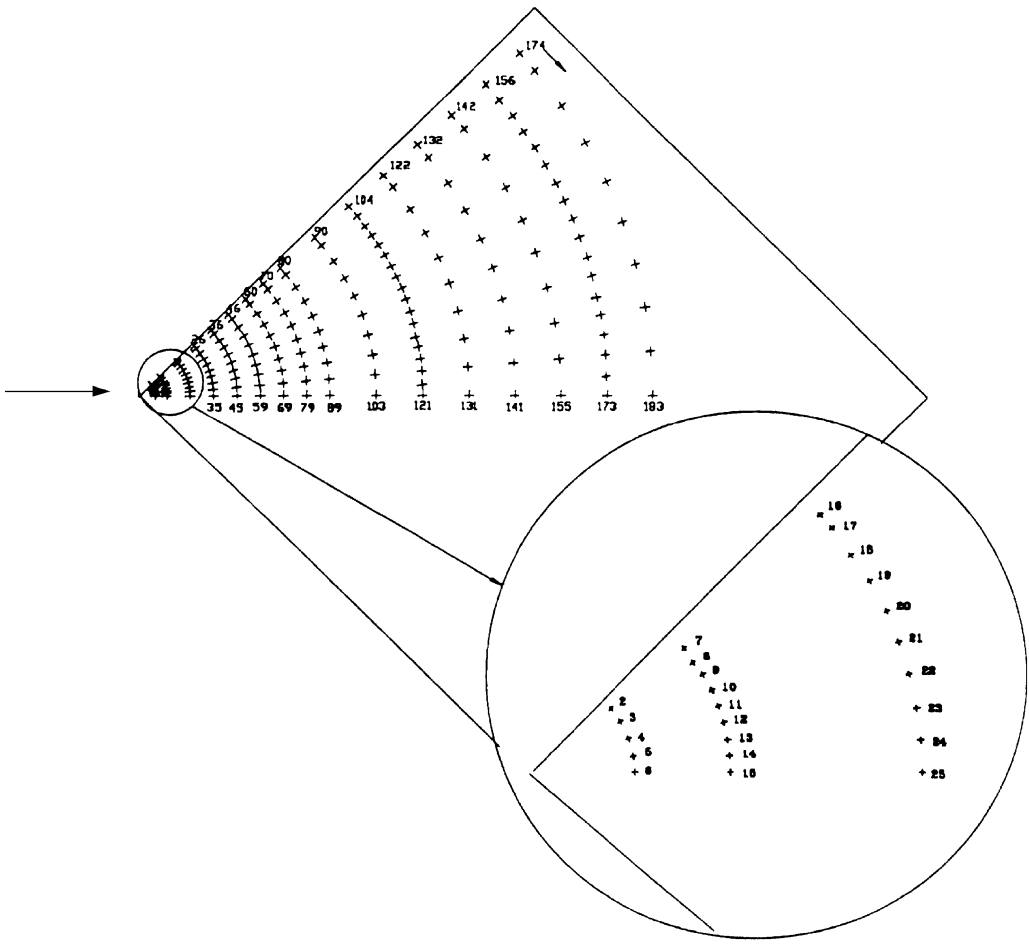

Figure 2. Location of pressure taps on the model of Williams (1995).

3.1.3. Results of Bienkiewicz & Sun (1992)

Bienkiewicz & Sun (1992) carried out tests on a 1/25th scale model of the Texas Tech University (TTU) building in the Colorado State University (CSU) $2{\cdot}1 \times 1{\cdot}8 \times 29$ m wind tunnel. The model is a cuboid ($\theta = 90^\circ$) with a slight roof pitch, with L = 0·552 m, W = 0·369 m and H = 0·156 m. The corner area was pressure tapped (Figure 3), and tests were carried out with and without parapets. However, the results with parapets are not considered here. The wind angle β was varied between -45° and $+45^\circ$ in 5° increments. The atmospheric boundary layer simulation that was used had a power law exponent of 0·14 and a turbulence intensity of 0·2 at the model roof height. Mean and peak pressure coefficients are presented, normalized with the mean velocity at roof height. The data was filtered at 200 Hz, so the peak values correspond to approximately 0·005 s samples.

3.2. Verification; The Data of Tieleman *et al.* (1994)

Tieleman *et al.* (1994) presents the results of pressure measurements made on 1/50th and 1/100th scale models of the TTU building in the University of Western Ontario (UWO) and CSU wind tunnels, with a wide range of turbulence intensities in the atmospheric boundary layer simulations. They again present results for mean and peak values (sample length 0·007–0·01 s) normalized with the mean velocity at the top of the building. In particular, they provide detailed data for $\beta = 15^\circ$, $\alpha = 28^\circ$ (below the vortex centre) with roof height turbulence intensities between 0·061 and 0·323. The results of Cook's model will be compared directly with this data, using the parameters derived form the datasets of Section 3.1.

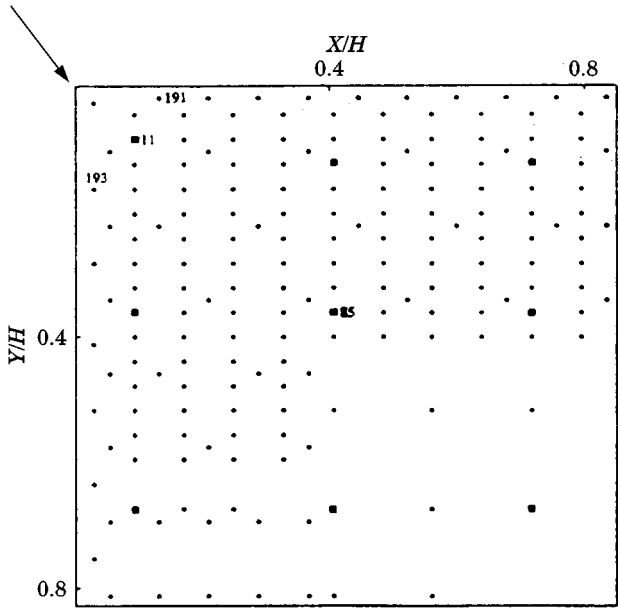

Figure 3. Location of pressure taps on the model of Bienkiewicz & Sun (1992); black squares indicate pressure taps on full scale TTU building.

4. THE MATURE REGION

As the first step in the verification of Cook's model we shall firstly consider the mature region. From equation (2) it can be seen that, if such a region exists, then the pressure along a line parallel to the edge of the building should be constant. The results of Williams (1995) allow a direct check to be made on this. Figure 4 shows some of Williams' data for mean pressure coefficient with $\beta = 0^\circ$, plotted in this way. It can be seen that the pressure becomes constant only on the leeward part of the roof upper surface for large values of L/H, and then only some distance inboard of the leading edge. Flow visualization data presented by Williams suggests that for the higher values of L/H the vortex core does not become parallel to the roof edge, but rather seems to drift towards the edge as the distance from the corner is increased. These results thus suggest that the mature region as defined by Cook does not in fact exist, at least for the range of experimental parameters investigated. In what follows that region will not be considered further. It is sufficient to state here that for high values of L/H the flow pattern changes in some fashion well away form the windward corner, but the nature of this change has not yet been elucidated.

5. THE GROWTH REGION

5.1. Determination of the Validity of the Growth Region Formulation

There are two basic tests to check whether the growth region formulation is adequate. The first is to plot the pressure coefficient data against log r. An example of this for the results of Williams is shown in Figure 5. It can be seen that, in general, the plots are straight lines and

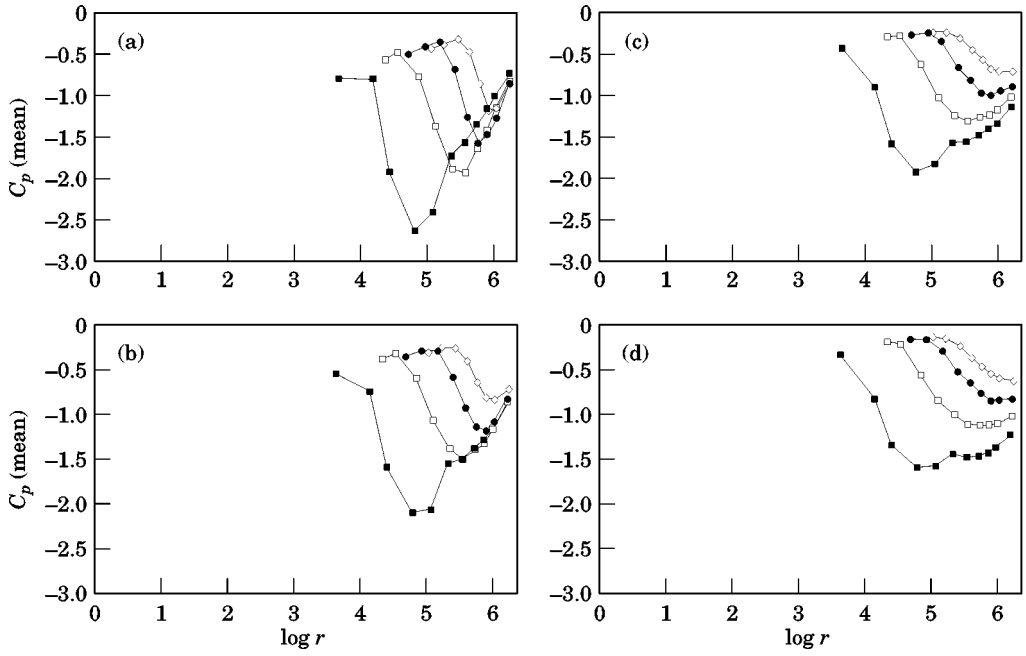

Figure 4. Data from Williams (1995) showing mean pressure coefficients plotted along lines a constant distance from the upstream edge of the block ($\theta = 90^\circ$, $\beta = 0^\circ$): (a) $L/H = 1$; (b) $L/H = 2$; (c) $L/H = 3$; (d) $L/H = 4$), r in mm. Distance from leading edge: (■) 25 mm; (□) 50 mm; (●) 75 mm; (○) 100 mm.

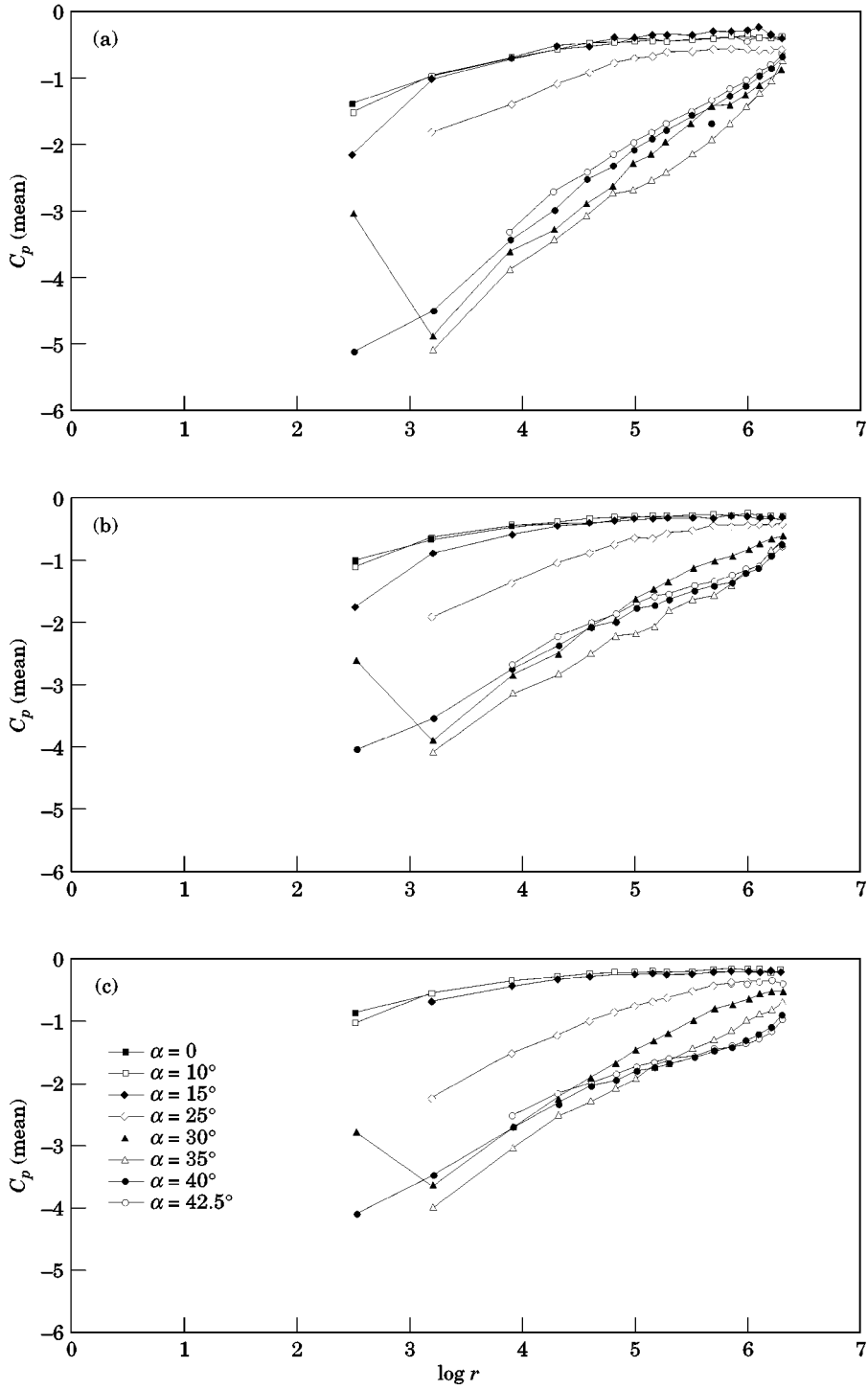

Figure 5. Data from Williams (1995) showing mean pressure coefficients plotted along lines of constant α; r in mm ($\theta = 90°$, $\beta = 0°$): (a) $L/H = 1$; (b) $L/H = 2$; (c) $L/H = 3$. (—■—) $\alpha = 0$; (—□—) $\alpha = 10°$, (—◆—) $\alpha = 15°$, (—◇—) $\alpha = 25°$; (—▲—) $\alpha = 30°$, (—△—) $\alpha = 35°$, (—●—) $\alpha = 40°$; (—○—) $\alpha = 42{\cdot}5°$.

are thus consistent with Cook's model, particularly for values of α greater than about 25°, which, it will be seen, corresponds with the region of the vortex core. It was further found that for nearly all the results considered the growth region formulation was applicable to nearly all the roof surface. It is of interest to note here that at the pressure tap nearest the leading edge, for $\alpha = 30°$ (near the vortex core), there is a low magnitude of C_p, which possibly represents a very small vortex development region.

Secondly, if the gradients of these lines (g) are plotted as a function of α they should have the form $g = -G/\{1 + [(\alpha - \alpha_0)/\alpha_c)^2]\}$ (see equation (3)). This is sketched in Figure 6. This procedure was carried out for the three datasets outlined in Section 3.1, and typical results from the data of Williams are shown in Figure 7 for the windward side of the roof only. From the results it is possible to derive validity tables showing the parameter range over which the growth region formulation is acceptable. Table 1 shows the results for the data of Maruta. The nomenclature used in this table is that, for each pressure coefficient type (mean or class A), and each wedge angle θ, a two letter code is given for each value of wind direction β: "WL" indicates that the tests just outlined indicate a vortex on the windward and leeward sides of the roof (Figure 1); "WX" indicates that a vortex is only observed on the windward side; and "XX" indicates that the pressure coefficients were not consistent with the pressure of vortices. From this table it can be concluded that in general the growth region model is valid for wedge angles (θ) greater than or equal to 60°, with vortices on the windward side for β up to 30°; and vortices on both windward and leeward sides for β up to 15°. There is a tendency for "mean" vortices to exist to higher values of β than "extreme" vortices.

Table 2 shows a similar tabulation for the results of Williams. The nomenclature is similar to that of Table 1, but different values of L/H are given, and the code "W?" indicates

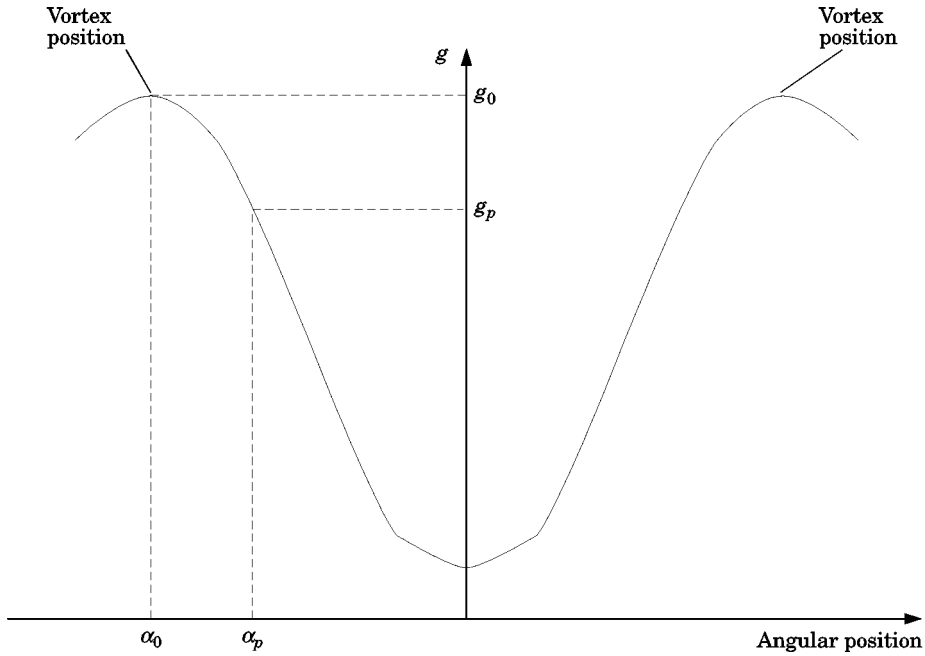

Figure 6. Expected variation of g with α of model is valid.

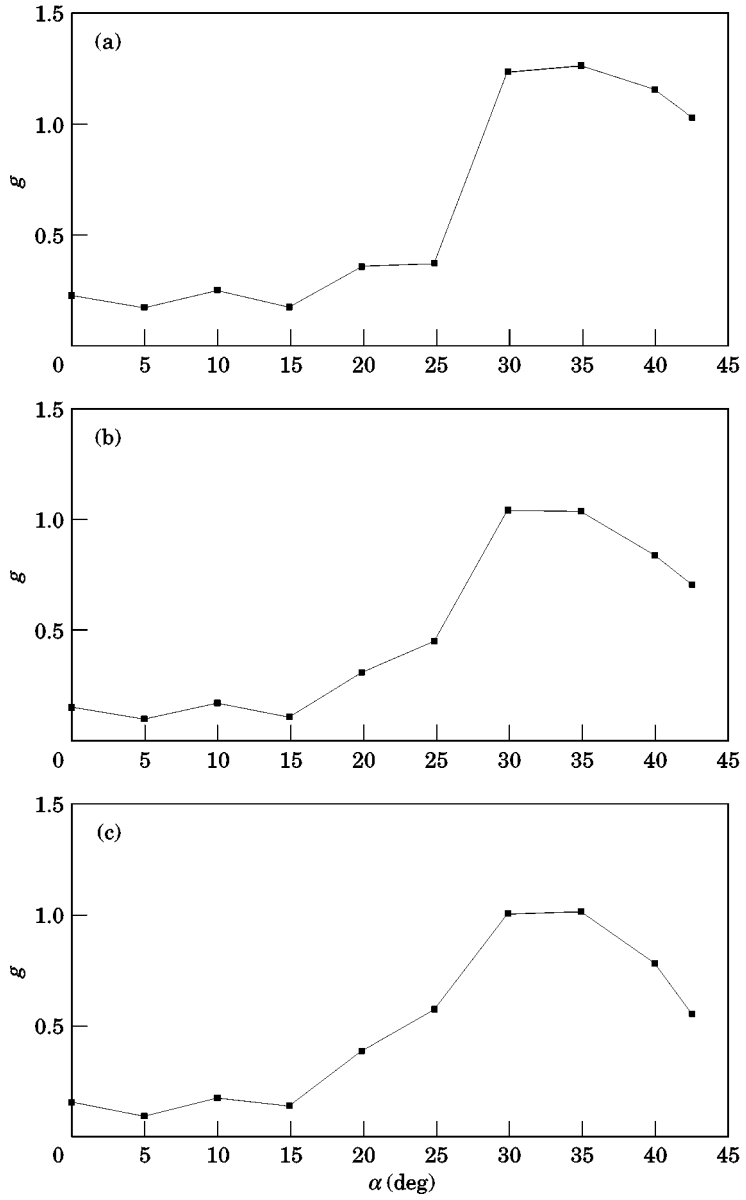

Figure 7. Data of Williams (1995) for g (mean pressures) against α ($\theta = 90^\circ$, $\beta = 0^\circ$): (a) $L/H = 1$; (b) $L/H = 2$; (c) $L/H = 3$.

vortices were observed on the windward side of the roof, and no data was available on the leeward side. The results are broadly consistent with Table 1 and show the validity of the formulation for the range of parameters considered.

Finally, Table 3 shows a similar tabulation for the results of Bienkiewicz & Sun (1992). Again, the results are broadly consistent, with "mean" vortices existing for β up to 20° and "extreme" vortices for β up to 10°. In conclusion, it would seem that for $\theta = 90^\circ$ (a cuboid,

TABLE 1
Validity of growth region formulation-data of Maruta (1985), $L/H = 1$

β°	θ°			
	30	0	90	120
Mean values				
0	XX	WL	WL	WL
15	XX	WX	WL	WL
30	XX	WX	WX	WL
45	XX	XX	XX	
60	XX	XX		
Class A				
0	XX	WL	WL	WL
15	XX	WX	WX	WL
30	XX	XX	WX	XX
45	XX	XX	XX	
60	XX	XX		

XX: no vortices; WL: vortices on windward and leeward sides of roof; WX: vortex on windward side only; blank: no data available.

TABLE 2
Validity of growth region formulation-data of Williams (1994), $\theta = 90^\circ$

β°	L/H			
	1	2	3	4
Mean values				
0	W?	W?	W?	W?
15	W?	W?	W?	W?
Class A				
0	W?	W?	W?	W?
15	W?	W?	W?	W?

W? indicates vortex on windward side, no data on leeward side.

by far the most common case), the growth region model of Cook is valid for wind angles β less than about 20° for mean pressure coefficients, and wind angles of less than about 10–15° for extreme pressure coefficients.

5.2. Determination of Growth Region Parameters

Cook determined the parameters in the model by an iterative best fit analysis of the data. This produced reasonable values for some of the parameters, but unrealistic values for the others. For example, he obtained values of the vortex core radius for a cuboid of between 40 and 70°. The approach taken here is rather different. Firstly, for each set of data a graph of the form of Figure 7 is produced. The vortex core position α_0 is then read directly from the graph. For $\alpha = \alpha_0$ the magnitude of the peak of the curve g_0 is simply equal to $-G$, (see equation (3)). Now suppose a point on the graph with $\alpha = \alpha_0$ is defined at which

TABLE 3
Validity of growth region formulation-data of Bienkiewicz & Sun (1992), $\theta = 90^\circ$.

β°	Mean pressures	Peak pressures
− 45	XX	XX
− 20	WL	XX
− 15	WL	XX
− 10	WL	WL
− 5	WL	WL
0	WL	WL
5	WL	WL
10	WL	WL
15	WL	XX
20	WL	XX
45	XX	XX

Key as for Table 1.

$g = g_p = pg_0$, where p is around 0·5; then, it is straightforward to show that

$$\alpha_c = (\alpha_p - \alpha_0)/\sqrt{(1/\mathrm{p}) - 1} \tag{4}$$

Thus, if p is exactly 0·5, $\alpha_c = \alpha_p - \alpha_0$.

Now, it is also possible for each set of data to draw a graph similar to Figure 7 that shows the values of the C_p versus log r graphs when $r = b$, the reference height, i, against angular position α. From this graph it is possible then to find values of i at $\alpha = \alpha_0$ and at $\alpha = \alpha_p$, i_0 and i_p. Again, it is simple to show that

$$C_{p0}(pi_0 - i_p)|(p - 1) \tag{5}$$

and

$$\Delta C_p = [-i_0 + i_p + (p - 1)g_0 \log b]/(p - 1) \tag{6}$$

Thus, values of the parameters in Cook's model can be calculated directly. We will now consider the results of such an analysis applied to the three basic data sets. In what follows, the reference length b is taken as the height of the building, H. It was found that this produced more consistent values of the parameters than the block height L, perhaps unsurprisingly, as H is the only scaling length that can be of relevance near to the windward corner. Similarly, the reason for rewriting equation (1) in the form of equation (3) was because the calculated parameters were less sensitive to precise details of the curve fit if this formulation was used. The results are shown in Figures 8–12 for the parameters α_0, α_c, C_{p0}, ΔCp and G, respectively. The results of Maruta for $L/H = 1$ are shown for class A and the mean pressure coefficients with $\beta = 0$ and 15° on the windward side of the roof, against wedge angle θ. The results of Williams for $\theta = 90^\circ$ are also shown for the mean and class A pressures for $\beta = 0$ and 15° on the windward side of the roof, but are tubulated against L/H and turbulence intensity at roof height I, these two parameters varying together for these results. The results of Bienkiewicz & Sun for $\theta = 90^\circ$ for mean and peak pressure coefficients on both the windward and the leeward side of the roof are tabulated against wind angle β.

5.3. Discussion of Results and Physical Interpretation of Growth Region Parameters

Firstly, consider the results in Figure 8 for α_0. From Figure 8(a) it can be seen that, as would be expected, α_0 increases as the wedge angle increases, but there seems to be little consistent variation with β, and the results are similar for mean and peak pressure coefficients. It will be seen in what follows that in general the results of Maruta are the most scattered and reveal little consistent variation, probably because of the rather restricted number of pressure tappings used in his experiments. The results of Figure 8(b) for $\theta = 90^\circ$ (which are only accurate to the nearest 5°) show the variation with L/H or turbulence intensity I, these two parameters being varied together in the experiments of Williams. These results suggest that α_0 decreases slightly as β increases, with the mean values being greater than the class A values, i.e. the extreme vortices lie in board of the mean vortices. Figure 8(c) shows the variation of α_0 with wind direction β. This figure for windward and leeward vortices should be symmetrical about $\beta = 0$. The results, however, suggest symmetry about a value of β rather less than 0, presumably because of a slight asymmetry in the experiments. The same effect will be seen in the figures that follow. Again, the results suggest for the windward vortices that α_0 decreases slightly as β increases, with the extreme values rather lower than the mean values. Now the extreme values of the pressure coefficients are obtained from an analysis of the time histories of pressures at individual points. Thus, the overall extreme pressure distribution does not correspond to an instantaneous data set. Now, the results of Kawai & Nishimura (1994) and Marwood *et al.* (1994) suggest that the delta wing vortices are oscillatory and intermittent. The analysis presented here suggests that, whilst on average a certain value of α_0, the vortex centre, can be identified, the vortex is strongest at that portion of its oscillatory cycle corresponding to the value of α_0 for the extreme distribution.

Figure 9 shows the results for α_c Figure 9(a) shows little consistent variation of this parameter with wedge angle; i.e. the size of the vortex core does not depend on wedge angle. Also, little variation can be seen between peak and class A values, or with wind direction. Figure 9(b) shows the variation of α_c with L/H and I. It can be seen that α_c increases with L/H or I, with wind direction β, and the class A values are greater than the mean values. The latter two trends can also be seen in the data of Figure 9(c). Thus, it would seem that the vortex core radius increases as the wind angle and the turbulence intensity increases. The large values for the extreme values probably again reflect the oscillatory nature of the vortex core, i.e. the movement of the vortex produces a larger effective core.

Figure 10 shows the variation of the reference pressure parameter C_{p0}. Figure 10(a) shows little consistent variation with wedge angle. Figure 10(b) shows that C_{p0} increases with L/H or I and perhaps with wind angle β, with the class A values being above the mean values. The same trends can be observed in the data of Figure 10(c), but the magnitudes of the parameter in Figure 10(b) and 10(c) do not compare particularly well. This is perhaps due to the common difficulty in wind tunnel testing of adequately specifying a reference static pressure, and some pressure offsets between different experiments are to be expected. It is also probably due to the different definitions of pressure coefficients for the extreme data.

Figure 11 shows the results for ΔC_p. Again, the results of Mauta in Figure 11(a) show little consistent variation with wedge angle. The results of Figure 11(b) show a general trend for the magnitude of ΔC_p to decrease with L/H or I increasing. Figure 11(c) shows an increase in this parameter with β for the windward vortex, again with the values corresponding to the peak pressures being greater than those corresponding to the mean pressures. Again, there is some discrepancy between the magnitudes of the results of

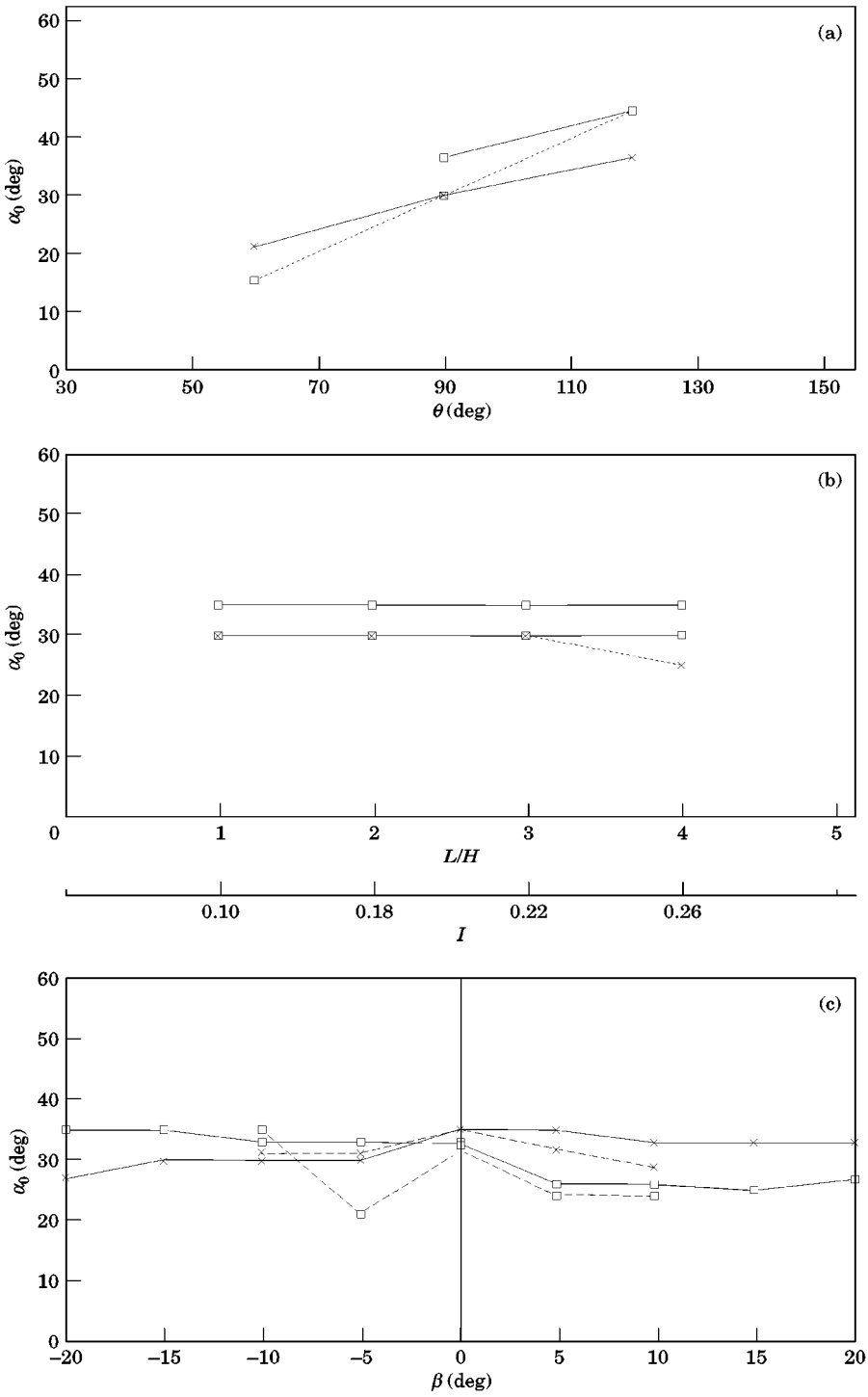

Figure 8. Calculated values of α_0: (a) results of Maruta; (b) results of Williams; (c) results of Bienkiewicz & Sun. (a) (—○—) Mean $\beta = 0°$; (— × —) mean $\beta = 15°$; (- -□- -) Class A $\beta = 0°$, (- - × - -) Class A $\beta = 15°$. (b) Key as for (a). (c) (—□—) Mean W, (— × —) mean L, (- -□- -) peak W; (- - × - -) peak L.

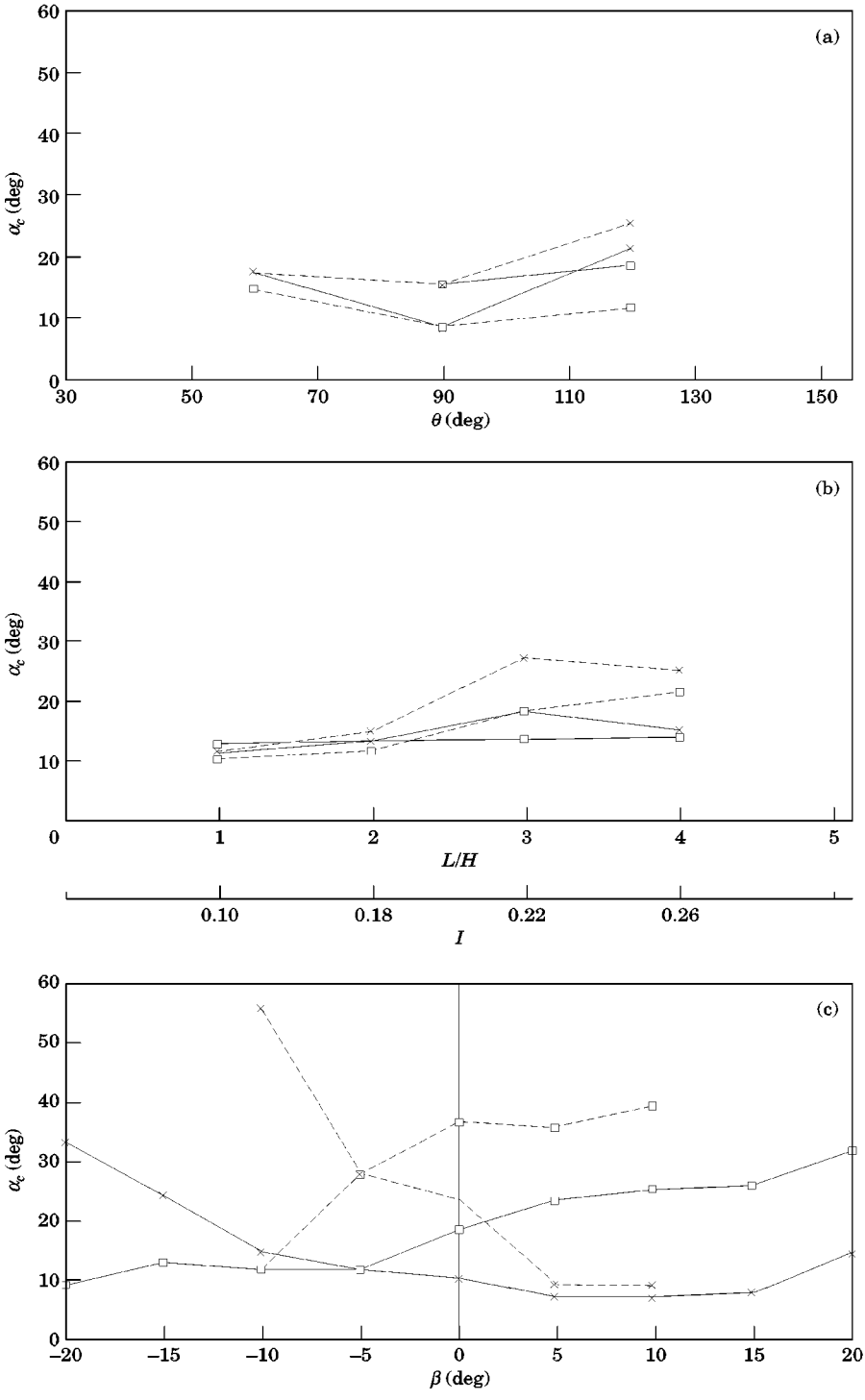

Figure 9. Calculated values of α_c: (a) results of Maruta; (b) results of Williams; (c) results of Bienkiewicz & Sun. Key as for Figure 8.

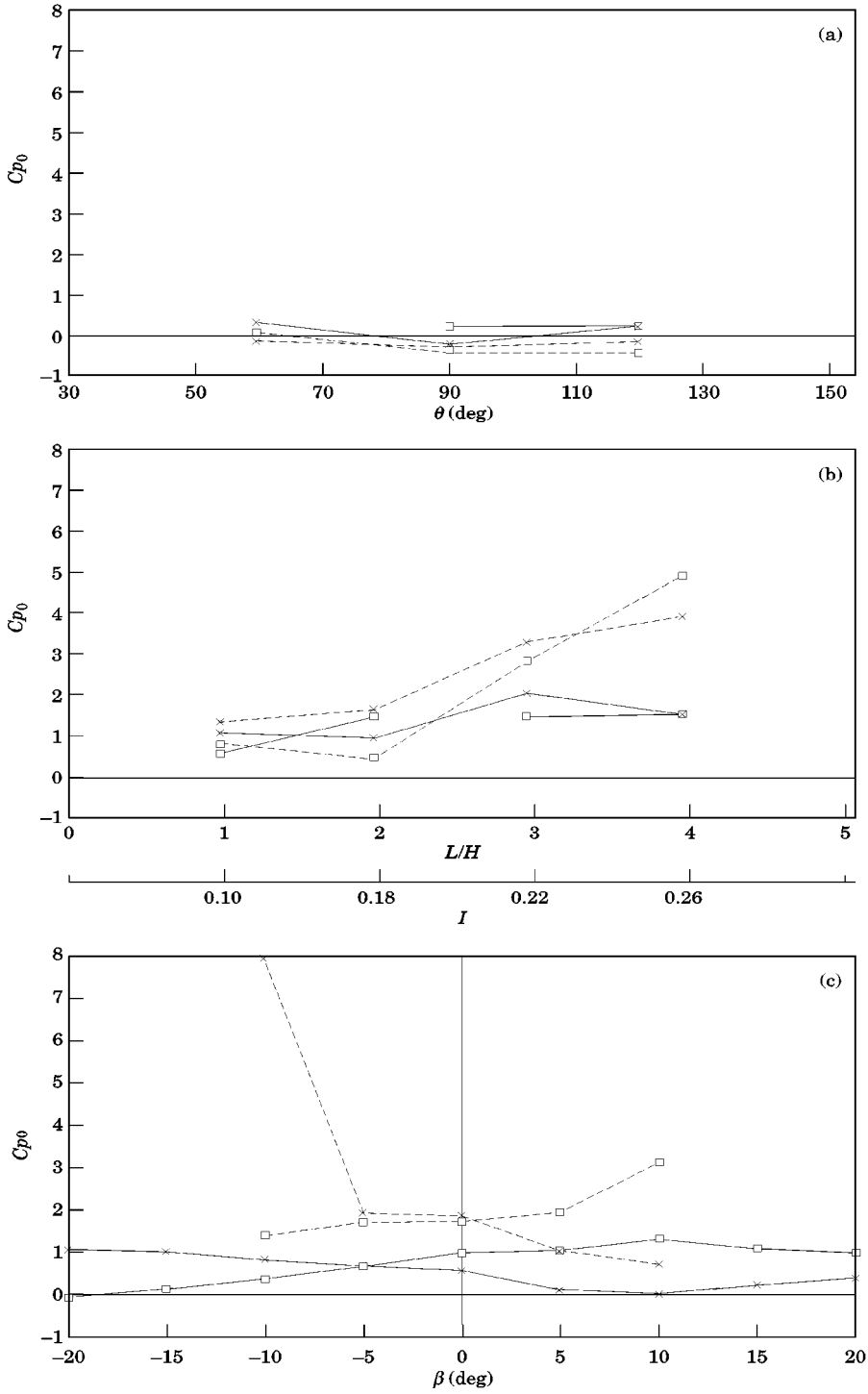

Figure 10. Calculated values of C_{p0}: (a) results of Maruta; (b) results of Williams; (c) results of Bienkiewicz & Sun. Key as for Figure 8.

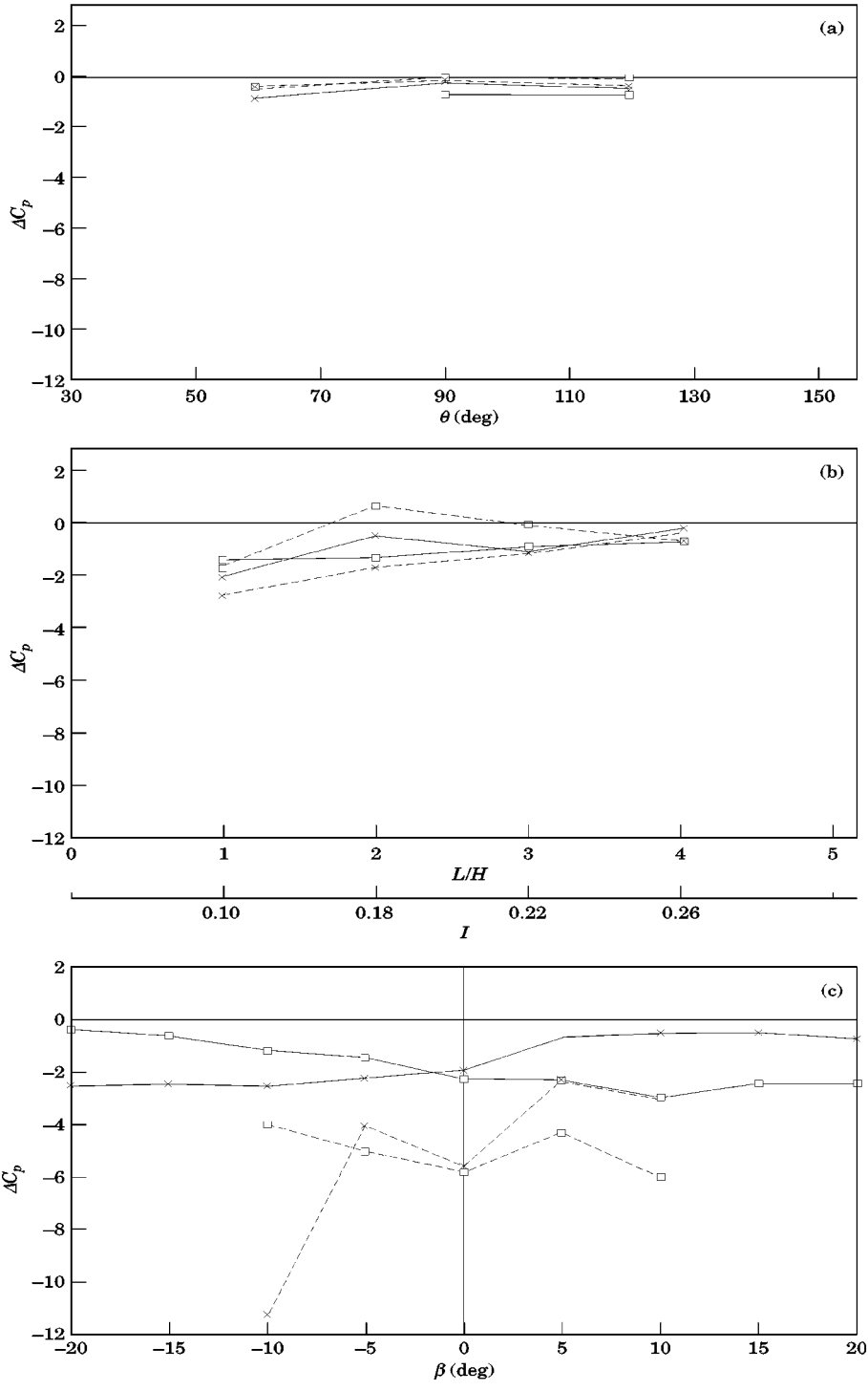

Figure 11. Calculated values of ΔC_p: (a) results of Maruta; (b) results of Williams; (c) results of Bienkiewicz & Sun. Key as for Figure 8.

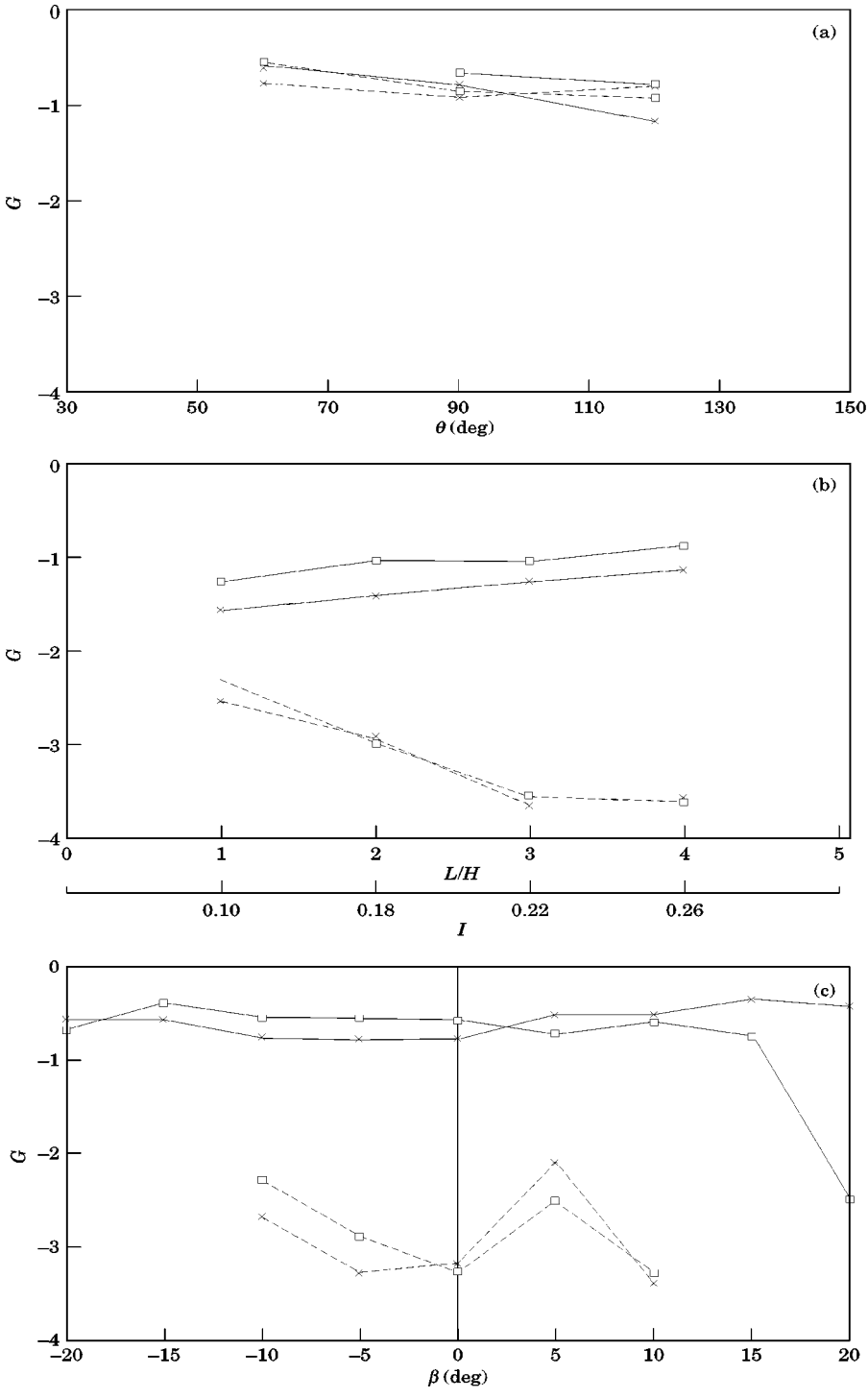

Figure 12. Calculated values of G: (a) results of Maruta; (b) results of Williams; (c) results of Bienkiewicz & Sun. Key as for Figure 8.

Figures 11(b) and 11(c), probably for the reasons outlined above. Physically these results imply a greater lateral variation of pressure coefficients for the class A peak results than for the mean results.

Finally, Figure 12 shows the results for the gradient parameter G. Figure 12(a) shows little effect of wedge angle. Figure 12(b) shows values of G of around $-1{\cdot}0$ for mean pressures,

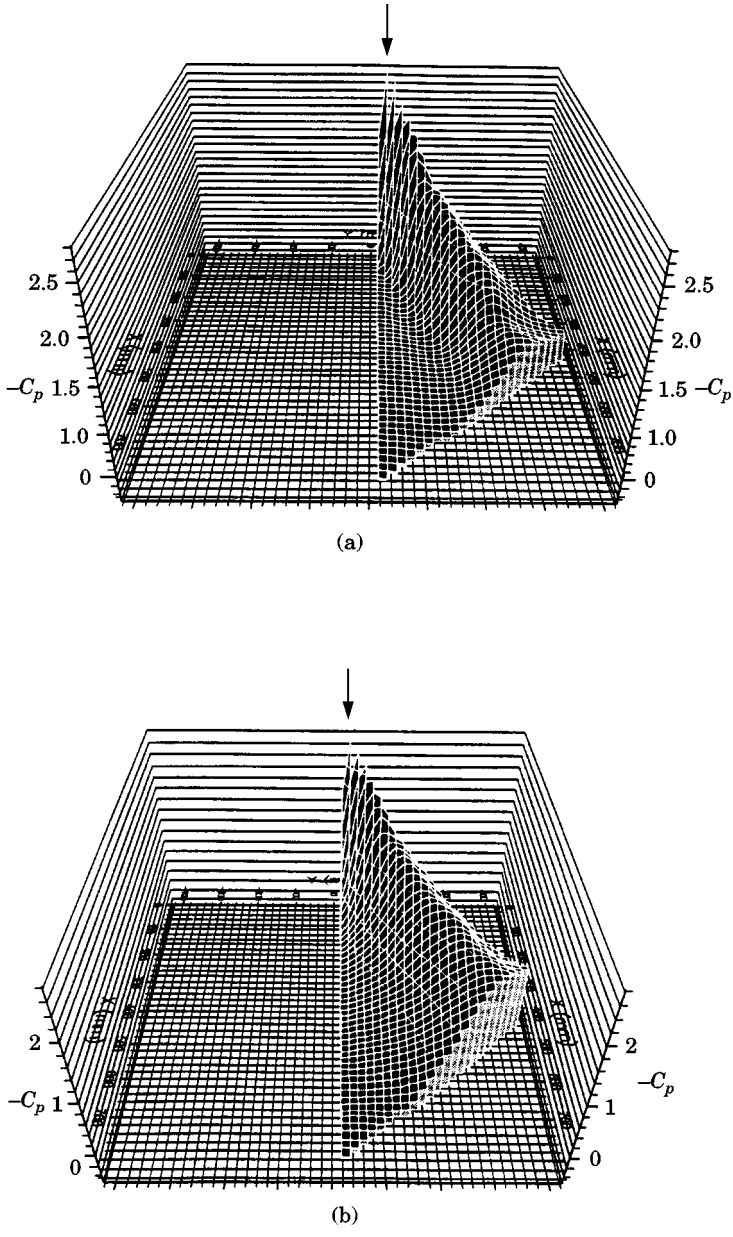

Figure 13. Data of Williams (1995). Back prediction of mean pressure coefficient ($\theta = 90^\circ$, $\beta = 0^\circ$, $L/H = 1$): (a) experimental, (b) predicted.

and around -3 for extreme pressures. Figure 12(c) shows slightly lower values of G for mean pressures (around $-0{\cdot}5$ to $-0{\cdot}7$), but similar values for extreme pressures. In physical terms, these results imply that the extreme pressures decay more rapidly than the mean pressures away from the leading corner.

Before concluding this discussion of the model parameters, it is of course possible to use the calculated parameters to "back predict" the experimental data. The results of such a procedure are shown in Figure 13 for some of the results of Williams. The predicted and the measured values can be seen to be of the same form. In general, Williams showed that the largest errors are in the roof regions, well away from the vortex core or towards the rear of the roof, as would be expected. However, in these regions the pressure coefficients are usually small and not of significance in design.

6. VERIFICATION OF PARAMETERS

In this section the model parameters obtained in section 5 are used to predict the pressure distributions measured by Tieleman *et al.* (1994) on the TTU building. Two predictions are carried out.

(a) Using the values in Figure 8–12 obtained from the data of Williams (1995), the mean and peak values of pressure coefficient for $\theta = 90^\circ$, $\beta = 15^\circ$ and $\alpha = 28^\circ$ (close to the vortex core) are calculated for different values and I. This assumes that the parametric variation is due to variations in I rather than L/H in this data. The comparison with the mean values of Tieleman *et al.* is straightforward, but the extreme values present some problems in view of the different definitions of extreme values used.

(b) Using the values in Figures 8–12 obtained from the data of Bienkiewicz & Sun (1992), the mean values of pressure coefficient for $\theta = 90^\circ$, $\beta = 15^\circ$ and $\alpha = 28^\circ$ were calculated for a value of I of 0·2.

Consider first the results of prediction (a). Figure 14(a) shows the mean value results of Tieleman *et al.* with C_p plotted against $\log_0(r/H)$ for $0{\cdot}61 < I < 0{\cdot}323$. The predicted results for $0{\cdot}1 < I < 0{\cdot}26$ are shown in Figure 14(b). The results can be seen to be in good qualitative agreement. The major discrepancy seems to be the positive values of C_p predicted for high I and high r/H. This is probably due to the problem in ensuring consistent static pressure measurements referred to in the last section. The general variation with I is well predicted.

Figures 15(a) and 15(b) show corresponding results for extreme values. In both cases, rather smaller variations with I can be seen than for the mean results. In general predictions are substantially lower in magnitude than the measured values. This is primarily due to the different definitions of extreme pressure coefficient used by Tieleman *et al.* and Williams. Tieleman *et al.* defined the extreme pressure coefficients as the ratio of extreme pressures to mean dynamic pressures, whilst Williams defined them as the ratio of extreme pressure to extreme dynamic pressures. If the predicted values, which are based on parameter values obtained from the latter data set, were to be multiplied by the square of the velocity gust factor, closer agreement would be obtained. Unfortunately, however, values of this parameter were not obtained in the investigation of Williams (1995).

Figure 16 shows the results of comparison (b) for mean pressure coefficients. The predicted results for $I = 0{\cdot}20$ are compared with the results of Tieleman *et al.* for $I = 0{\cdot}195$. Against, there can be seen to be reasonable agreement, but with an offset that may be partly due to static pressure definition problems.

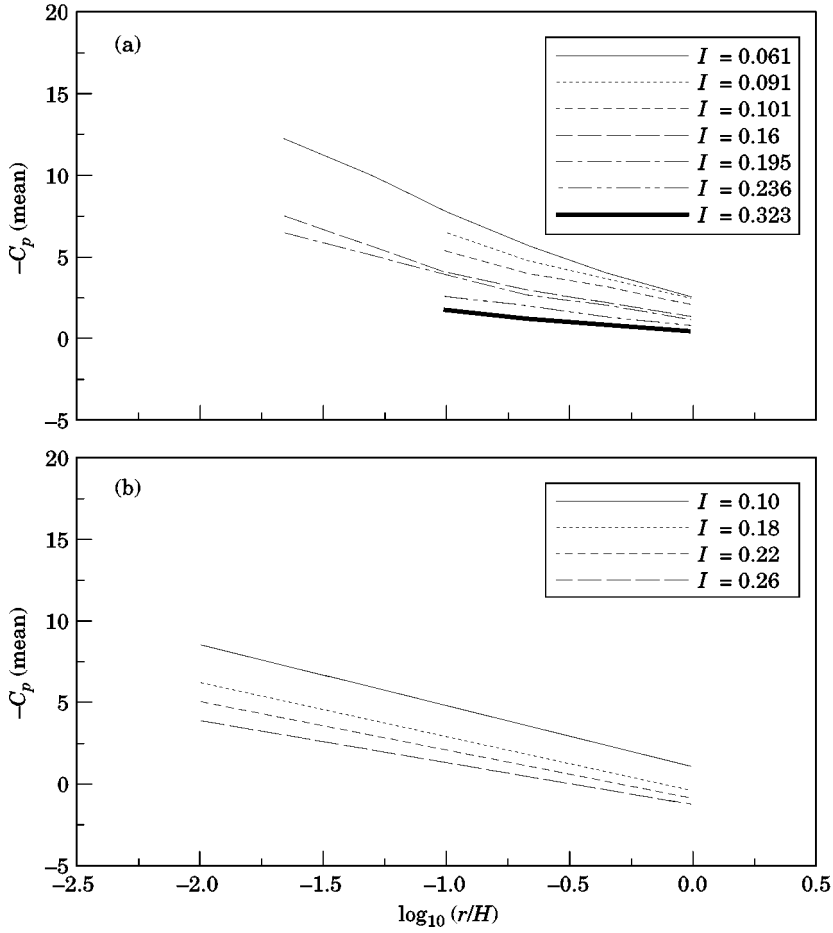

Figure 14. Verification of model for $\theta = 90°$, $\alpha = 28°$, $\beta = 15°$: (a) Tieleman *et al.* mean pressures; (b) model predictions for mean pressures.

7. DISCUSSION AND CONCLUDING REMARKS

Before proceeding to draw together the work of previous sections, it is worth describing in a little more detail the results of two investigations already mentioned briefly: those of Marwood *et al.* (1994) and Kawai & Nishimura (1994). Both these investigations show quite clearly that the delta wing vortex flow is essentially unsteady. Marwood *et al.* suggest from LDA measurements that his unsteadiness is primarily due to an intermittency of the flow, whilst Kawai & Nishimura suggest from an analysis of surface pressure correlations that there is a regular oscillatory flapping of the vortex system. These two observations are not, of course, mutually exclusive. In addition, the pressure spectra of Williams (1995) showed low frequency peaks which could be attributed to such an intermittency or vortex flapping. Thus, mean pressure fields represent the mean of an unsteady system of vortices moving over the roof, whilst extreme pressure fields, usually measured by extreme value analysis of sequential measurements of pressure at individual pressure tappings, represent simply the

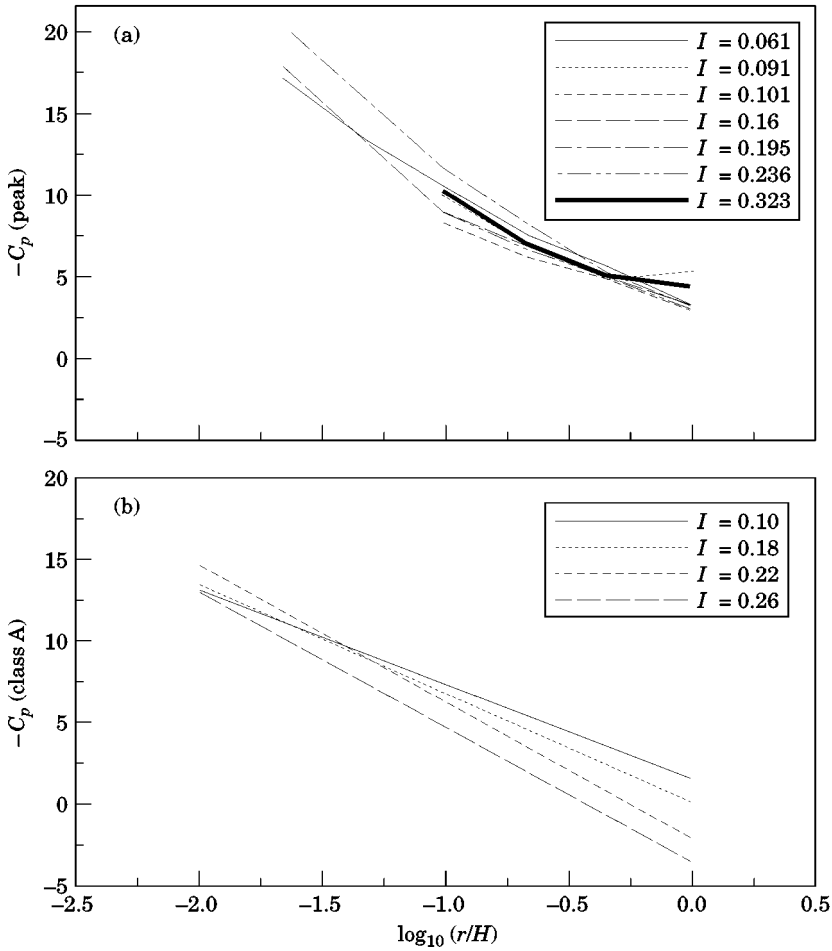

Figure 15. Verification of model for $\theta = 90°$, $\alpha = 28°$, $\beta = 45°$: (a) Tieleman *et al.* mean pressures; (b) model predictions for mean pressures.

extremes registered at each point, which may well be measured at different parts of the oscillatory cycle for different points. It is worthwhile to bear this point in mind in the discussion that follows.

Firstly, consider the validity of Cook's model. Very broadly, it would seem that the growth region model is an adequate representation of the surface pressure field for included building angle $\geq 60°$, with a wind direction of approximately $\pm 15°$ from the corner bisector, this angle being rather less for extreme pressure fields than for mean pressure fields. The mature region model proposed by Cook does not appear to be adequate, although these is some evidence from the results of Williams (1995) to suggest that there is a change in flow pattern at the rear of the roof for low height/length ratios, with the vortices appearing to move towards the roof edge. This is further supported by the flow visualization of Kramer & Gerhardt (1991) and the expression for pressure variation with r given by Tieleman *et al.* (1994), where C_p is taken to be given by an expression of the form

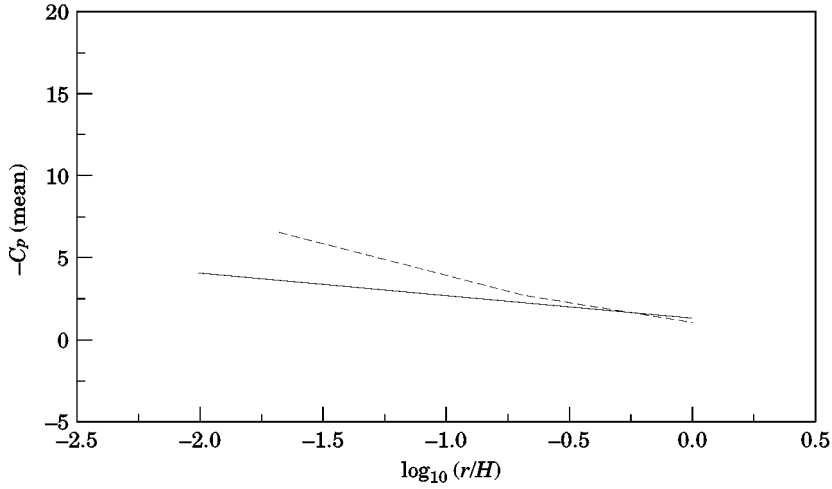

Figure 16. Verification of model for $\theta = 90°$, $\alpha = 28°$, $\beta = 45$. Mean pressures; results of Tieleman *et al.* and model predictions: (——) predicted, $l = 0{\cdot}2$; (- - -) measured, $l = 0{\cdot}195$.

$\{a + b \log r + c(\log r)^2\}$, i.e. a deviation from the expression suggested by Cook for large r. Further work is needed to elucidate the nature of the flow in this region.

For the growth region the predicted parameter values are on the whole consistent between the data sets, particularly for the vortex parameters α_0 and α_c. As is expected, the vortex position α_0 is different for extreme and mean pressure fields, reflecting the oscillatory nature of the flow. α_c, the vortex width, increases with turbulence intensity, perhaps indicating an increasing oscillatory nature, and is greater for the extreme pressure fields, reflecting a broadening of the effective vortex width. However, the discussion above needs to be borne in mind—it may be that the measured extreme pressure field only poorly describes the real nature of the flow.

The parameters C_{p0}, ΔC_p and G are also generally consistent, but the results for the various data sets differ somewhat, probably due to the different definitions of the pressure coefficients used by the investigators, and due to the problem in defining static pressure.

Now, if the model is to be of use in design, it is important that near the windward corner (say $r/H = 0{\cdot}1$) the values of C_p should be predicted to a certain accuracy; $\pm$ 10% seems reasonable. For this value of r/H, at the vortex centre ($\alpha = \alpha_0$), for $\theta = 90°$, $\beta = 10°$ it is easily shown from equation (3) that

$$\frac{dC_p}{dC_{p0}} = 1, \qquad \frac{dC_p}{d\Delta C_p} = 1, \qquad \frac{dC_p}{dG} = 2{\cdot}30, \tag{7}$$

Thus, for C_p to be accurate to within $\pm$ 10%, C_{p0} and ΔC_p needs to be accurate to this level, and G needs to be accurate to $\pm$ 4·3%. From Figures 10–12 it can be seen that it would at present be difficult to specify these parameters to this level of accuracy. Thus it would seem that at present the model is probably not adequately specified for design purposes. More work is needed to determine the various parameters for different values of turbulence intensity, wind angle, etc. It may well be that sufficient data already exists in the literature to enable this to be done–for example, only some of the extensive data of Tieleman *et al.* (1994)

has been used here, but this represents a considerable data analysis task. It seems likely that, for the immediate future, the main use of the model will be as a research tool, to provide a framework for the investigation and parameterization of delta wing vortex systems.

As an example of such a use, it is of interest to consider how the model can be used to predict area averaged pressures. It can easily be shown from an area integration of equation (3) that, for an area of radius R from the windward corner for $\beta = 0^\circ$ (i.e. symmetric flow), the area averaged pressure is

$$C_{p0} + \left(\frac{4\alpha_c}{\pi}\right)\left(\Delta C_p - G\log\frac{R}{H} + \frac{G}{2}\right)\left[\tan^{-1}\left(\frac{\pi}{4\alpha_c} - \frac{\alpha_0}{\alpha_c}\right) - \tan^{-1}\left(\frac{\alpha_0}{\alpha_c}\right)\right.$$

Clearly, this simple case yields a simple analytical expression. However, in principle, the area averaged pressure over any part of the roof can be calculated from equation (3) for any wind angle, etc., although in general numerical techniques will need to be used for this. Also, in view of what was said earlier, this approach is only valid for mean pressure fields–area averaged extreme pressure fields depend upon both the spatial and time dependence of surface pressures. For applications such as this the parametric model is an extremely useful tool.

ACKNOWLEDGMENTS

This work described in this paper was carried out under a BRE extra mural contract, and the help and advice of Prof. N. Cook and Dr P. Blackmore at BRE are gratefully acknowledged.

REFERENCES

BIENKIEWICZ, B. & SUN, Y. 1992. Local wind loading on the roof of a low rise building. *Journal of Wind Engineering and Industrial Aerodynamics* **45,** 11–24.

COOK, N. J. 1985 *The Designer's Guide to Wind Loading of Building Structures. Part 1*. London: Butterworths.

COOK, N. J. 1990 *The Designer's Guide to Wind Loading of Building Structures. Part 2: Static Structures*. London: Butterworths.

KAWAI, H. 1996 Structure of conical vortices related with suction fluctuation on a flat roof. In: *Proceedings Bluff Body Aerodynamics and Its Applications 3*, Blacksburg, Virginia, U.S.A.

KAWAI, H, NISHIMURA, G. 1994 Flow field and suction on a flat roof. In: *Proceedings 2nd Wind Engineering Society Conference*, Warwick.

KARMER, C. & GREHARDT, H. J. 1991 Wind pressures on roofs of very low and very large industrial buildings. *Journal of Wind Engineering and Industrial Aerodynamics* **38,** 285–295.

MARUTA, E. 1985 Wind pressure distributions on the roofs of wedge shaped models. BRE Internal Note N69/85.

MARWOOD, R., BELCHER, R. F., MINSON, A. J. & WOOD, C. J. 1994 Flow structures associated with extreme pressures on flat roofs. In: *Proceedings 2nd Wind Engineering Society Conference*, Warwick.

MARWOOD, R. & WOOD, C. J. 1996 Conical vortex movement and its effect on roof pressures. In: *Proceedings Bluff Body Aerodynamics and its Applications 3*, Blacksburg, Virginia, U.S.A.

THOMAS, G. & WILLIAMS, J. J. R. 1996 Development of a parallel code to simulate skewed flow over a bluff body. *In Proceedings Computational Wind Engineering Conference*, Fort Collins, Colorado, U.S.A.

TIELEMAN, H. W., SURRY, D. & LIN, J. Z. 1994 Characteristics of mean and fluctuating pressure coefficients under corner (delta wing) vortices. *Journal of Wind Engineering and Industrial Aerodynamics* **52,** 263–275.

WILLIAMS, C. W. 1995 A semi-empirical model for predicting wind loads on building roofs. Ph..D. Thesis, University of Nottingham, U.K.

APPENDIX 1: THE RANKINE VORTEX ABOVE A SURFACE

The tangential velocity within an isolated Rankine vortex core is given by

$$u = \left[2u_c\left(\frac{d}{d_c}\right)\right] \Big/ \left[1 + \left(\frac{d}{d_c}\right)^2\right] \tag{A.1}$$

where u_c is the tangential velociy at a distance $d = d_c$ from the centre of the vortex. Now, from equation (A.1) for a Rankine vortex at a height h above a surface, the velocity v parallel to the surace at a distance l from the normal to the surface through the vortex core is given by:

$$v = \frac{4u_c(h/d_c)}{1 + (l^2 + h^2)/d_c^2} \tag{A.2}$$

allowing for the image in the surface. Thus, the pressure coefficient corresponding to this, based on a reference velocity u_r, is given by

$$C_p = -\frac{(u_c/u_r)(4\bar{h})^2}{(1 + \bar{l}^2 + \bar{h}^2)^2} \tag{A.3}$$

where $\bar{h} = h/d_c$ and $\bar{l} = l/d_c$. Thus,

$$C_p = \left\{\frac{-16(u_c/u_r)\dfrac{(\bar{h})^2}{(1+\bar{h}^2)^2}}{\left((1 + \dfrac{\bar{l}^2}{1+\bar{h}^2}\right)^2}\right. \tag{A.4}$$

A comparison of this equation with equation (1) shows that the latter does not fully represent the pressure field of a Rankine vortex. If $(\alpha - \alpha_0)$ in equation (1) is taken to be equivalent to $\bar{l}$ in equation (A.4), i.e. the diminisionless distance from the vortex core, then an extra exponent of 2·0 is required in the denominator of equation (1) to be consistent with equation (A.4). It can also be seen that the parameters $\underline{b}$, α_c, C_{p1}, C_{p0}, S, etc. are in some sense surrogates for the more physically realistic parameters $\bar{h}(= h/d_c)$ and (u_c/u_r).

APPENDIX 2: NOTATION

b	reference length
C_p	pressure coefficient (mean or extreme)
C_{p0}	reference pressure coefficient, equation (1)
C_{p1}	reference pressure coefficient, equation (1)
g	gradient of C_p versus log r plot
g_0	g at $\alpha = \alpha_0$
g_p	g at $\alpha = \alpha_p$
G	gradient parameter equation (3)
H	block or building height
i	intercept of C_p versus log$r$ plot at $r = b$
i_0	i at $\alpha = \alpha_0$
i_p	i at $\alpha = \alpha_p$
l	turbulence intensity
L	building length
P	factor in parameter determination (Section 5.2)
r	distance from windward corner
r_m	value of r at start of mature region
R	distance from windward corner used in area averaging procedure
S	gradient parameter, equation (1)
W	building width
x	distance from windward corner (+ ve β)
y	distance from windward corner (− ve β)

y_0	vortex position in mature region
y_c	vortex size in mature region
α	angular displacement from bisector of windward corner (Figure 1)
α_0	angular position of vortex core in growth region
α_c	angular vortex size in growth region
α_p	value of α where $g = g_p = pg_0$
β	wind angle from bisector of windward corner (Figure 1)
ΔC_p	pressure difference parameter, equation (3)
θ	wedge angle